Alleviating Solar Energy Congestion in the Distribution Grid via Smart Metering Communications

Chun-Hao Lo, *Student Member*, *IEEE*, and Nirwan Ansari, *Fellow*, *IEEE*

Abstract—The operation and control of the existing power grid system, which is challenged with rising demands and peak loads, has been considered passive. Congestion is often discovered in high-demand regions, and at locations where abundant renewable energy is generated and injected into the grid; this is attributed to a lack of transmission lines, transfer capability, and transmission capacity. While developing distributed generation (DG) tends to alleviate the traditional congestion problem, employing information and communications technology (ICT) helps manage DG more effectively. ICT involves a vast amount of data to facilitate a broader knowledge of the network status. Data computation and communications are critical elements that can impact the system performance. In this paper, we consider congestion caused by power surpluses produced from households' solar units on rooftops or on ground. Disconnecting some solar units is required to maintain the reliability of the distribution grid. We propose a model for the disconnection process via smart metering communications between smart meters and the utility control center. By modeling the surplus congestion issue as a knapsack problem, we can solve it by proposed greedy solutions. Reduced computation time and data traffic in the network can be achieved.

Index Terms—Smart grid, cyber-physical system, demand and supply, distributed generation, renewable energy resources, power surplus, congestion, coordination and scheduling, smart metering.

✦

1 INTRODUCTION

THE electric power grid is one of the national critical infrastructures provisioned with reliability and security assurances. The existing grid is nearly a hundred year old, and many electric facilities and equipment in the grid are based on old technologies. While the power grid operation essentially entails voltage/current control as well as fault detection and isolation, most of research works on reliability of the power grid system have only focused on 1) the *current carrying* from power generation, transmission, to distribution lines consisting of numbers of transformers, buses, and circuit breakers, and 2) the *protection system* interacting with the current carrying methods that can be affected by the performance of protective relays, reclosers, and the associated hardware [1]. There have been a few research works on modeling telecommunications and distributed computing for the grid operation. As the smart grid vision has emerged, integrating information and communications technologies (ICT) into the power grid will provide greater transparency with data collection and aggregation throughout the entire network. More intelligent and automatic protection of the grid will be achieved with the aid of ICT

implementation. Meanwhile, the cyber-physical system will require preliminary investigations and analyses on communications network modeling, interoperability of various technologies, and vulnerability of the system, primarily instigated by cyber-security threats with respect to data protection and privacy [2], [3], [4], [5].

The conventional power grid has been built under a centralized infrastructure such that a single far-end power generator supplies power to multiple groups of end users through transmission and distribution lines. The centralized method has limited the improvement of system performance in terms of network availability and operational flexibility [6]. Meanwhile, the infrastructure is greatly vulnerable to single-point failures and attacks. Furthermore, according to the US Energy Information Administration (EIA) Annual Energy Review 2009 [7], the efficiency of the current power grid is as low as approximately 30 percent because of the loss in energy conversion at power plants and the loss in transmission and distribution.

Power transmission congestion has also been one of the major issues in the centralized power system network. According to the US Department of Energy (DOE) 2009 National Electric Transmission Congestion Study [8], the two most critical congestion areas are 1) midstate New York and southward along the Atlantic coastal plain to northern Virginia, and 2) the urban centers of southern California. Power flow in transmission lines often becomes congested when the network is overloaded due to rising power demand and power generation, insufficient capacity and capability of power transmission, peak demands in urban areas, distant demands in rural areas, and a lack of power transmission lines. In addition, abundant but intermittent

• *The authors are with the Advanced Networking Laboratory, Department of Electrical and Computer Engineering, New Jersey Institute of Technology, Newark, NJ 07102. E-mail: {cl96, nirwan.ansari}@njit.edu.*

power generation from renewable energy sources (RES) such as solar and wind farms raises even more challenges for network operators to control. Since there is not enough transmission capacity to support all demands for deliveries (transactions) that cannot be physically implemented as requested, congestion management methods are required for deregulated electricity markets [9], [10].

The smart grid vision initializes the transition from a centralized macrogrid to multiple decentralized microgrids (MGs) in order to enhance the quality and stability of energy distribution and decrease greenhouse gas emissions. The development of MGs tends to reduce long-distance power transmission losses and alleviate power congestion by balancing power supply and demand in a distributed way. An MG is a controlled and coordinated grouping of electrical *sources* and *loads* that operates in union as a single manageable entity. Electrical sources include distributed generation (DG) and energy storage, whereas loads refer to power demands. The MG is operated in two modes: grid-connected mode and islanded mode [11], [12]. In the grid-connected mode, power in MGs is supplied from both the main (macro) grid and its local DG. When an incident is detected (e.g., voltage drop, faults) in the main grid, MGs automatically switch to the islanded mode until the incident is resolved. Most research works have devoted to the islanded operation and the transition between islanded and grid-connected modes [13]. DG systems consist of diverse distributed energy resources (DER) technologies, such as solar panels, wind turbines, combined heat and power (CHP), MicroCHP, microturbines, and fuel cells. Many MG research, development, and demonstration activities are in progress throughout the world, e.g., the National Technical University of Athens (NTUA) in Europe and the Consortium for Electric Reliability Technology Solutions (CERTS) in US [11], [12]. The effectiveness of MGs along with DG implementation entails policies and regulations [14], control strategies and communications algorithms [15], and contribution factors in terms of real and reactive power flow analysis [13], [16]. They are all parts of smart grid projects.

The proliferation of DG deployed in MG and neighborhoods will further increase the penetration of DER and local generation capacity. Installing solar panels on rooftops of houses and buildings has dramatically increased recently in various countries. Consumers may use solar energy they produce from the solar units to operate their household appliances and personal electronics. Any extra energy that is unused will flow back to the utility grid for credits on their bills, i.e., in the case of a grid-tie system. Once DG becomes more prevalent in the future, congestion can potentially occur in the distribution grid [17]. The predicament is such that too much solar power or surge in solar power may incur local congestion and deterioration in power grids during both low consumption and intermittent generation periods. Bidirectional power flow in grid distribution has to be managed and monitored via smart metering communications (SMC) in order to avoid network congestion. The main contributions of this paper are summarized in the following:

- Congestion occurred in different situations in the power grid is presented and a number of strategies for mitigating the corresponding problems are discussed,

i.e., traditional congestion management methods and demand response approaches.

- The congestion problem due to a surplus of solar power in neighborhoods is defined and formulated as one type of knapsack problems (KPs). Selection techniques of disconnecting solar units are proposed.
- A framework of SMC using wireless technologies in the neighborhood area network (NAN) is provided, and a mechanism for exchanging data packets during the disconnection period is also proposed.
- Heuristic algorithms for unit selection are proposed based on greedy approaches. Simulations for determining the outcomes of the selection algorithms as well as upstream data traffic via SMC are conducted and discussed.

The remainder of this paper is structured as follows: Section 2 introduces methods of traditional power congestion control as well as several research works focused on demand response in home energy management and DER utilization. Section 3 presents a power system model where congestion due to solar surplus may occur in a neighborhood. It further describes the operation of a PV solar system and discusses means of disconnecting solar units from the distribution grid. A model for the disconnection process via SMC is also developed. Section 4 formulates the congestion problem and analyzes both dynamic programming (DP) and greedy approaches. Heuristic algorithms are proposed for unit (de)selection. Section 5 analyzes the simulation results of the proposed algorithms and discusses the findings. Finally, Section 6 summarizes the focal points and draws a conclusion.

2 BACKGROUND AND RELATED WORKS

Congestion management employed in the power grid system has been developed based on a number of methods, including spot pricing theory, optimization model, and variants of optimal power flow techniques [10], [18], [19]. While utilities tackle the congestion problem using their own rules and bidding strategies, all of them aim to maximize their profits (minimize overall cost) by using tools such as *unit commitment* and *economic dispatch* in the competitive electric industry [20]. Unit commitment refers to scheduling generation units to match the forecast load, whereas economic dispatch is adopted to meet the unexpected risen loads [21]. Essentially, *cost-free* methods[1] are first applied when congestion is revealed in the interconnected network. If congestion cannot be relieved, *not-cost-free* methods[2] are required to tackle the corresponding events [10], [18]. In either case, congestion management in power flow analysis is affected by both technical (security and stability) and economic (wholesale market price), which are usually contradictory.

---

1. Cost-free methods include outing congested lines and utilizing the flexible AC transmission system (FACTS) to manage the power flow. They are called cost-free because their marginal costs are nominal.

2. Not-cost-free methods include rescheduling and redispatching power generation in such a way that the power flow in transmission lines is more balanced throughout the network. This approach is more expensive because some generators may need to reduce their power generation while some are required to increase their output.

Traditional congestion management and control is considered to be *passive* since most methods focus on redispatching/rescheduling generation from the supply side. Congestion management will be more effective if demand control is combined with supply management [10], [16], [19]. In an analogy between supply and demand in power and communications networks, congestion control in the communications network effectively reduces senders' transmitting rates usually managed at the transport layer of the OSI model. In addition to assigning different costs or weights to the transmission lines/links or to meeting user demands in both systems, curtailing loads can dramatically improve system performance especially when a considerable amount of power and data flows is destined for the same destination and when resource is limited. In fact, various *demand response* programs in the smart grid projects are being deployed in the end-use sector including residential and commercial buildings [4], [6], [8].

An increasing number of research papers have focused on the implementation of energy management and scheduling techniques in houses and buildings [22], [23], [24], [25]. Shifting some major tasks of household appliances to off-peak periods and managing DER use efficiently during peak hours can achieve reduction in both energy cost and peak load. Erol-Kantarci and Mouftah [22] proposed a wireless sensor home area network (HAN) based on IEEE 802.15.4 to manage the time use of household appliances depending on the availability of its local energy. A simple communications protocol with an energy management unit (EMU) deployed in houses was developed. Prior to energy use by consumers, communications between the EMU and appliances as well as between the EMU and energy storage are established. Energy is granted if energy in storage is available. Consumers have the option whether to consume the grid power or not when energy in storage is insufficient. Mohsenian-Rad et al. [23] proposed a strategy that enables communications among households as a group demand-side management to minimize both energy cost and demand peak-to-average ratio. Local optimization using game theory to curb aggressive consumers is achieved. Similarly, Ibars et al. [26] identified a congestion game in demand and generation management as one of potential games in game theory. A load balancing mechanism was proposed to avoid power overload and outage by minimizing the cost (which is a function of the congestion level) on the flow along the transmission lines between a single generation and multiple consumers. Molderink et al. [24] proposed the three-step methodology (prediction, planning, and real-time control) to optimize the utilization of the grid power in a neighborhood by exchanging energy profiles among houses. Energy profiles are generated from local controllers installed in houses and aggregated for delivery to the global controller to make a global decision. Pedrasa et al. [25] proposed to maximize the profit of DER operation by scheduling DER in cooperation by using the particle swarm theory. Notably, congestion is also foreseen in plug-in hybrid electric vehicle (PHEV) charging if the charging management is not handled properly in the distribution grid. One way to mitigate the problem is to reduce the probability of overload by applying queuing theory [27]; balancing the charging loads over time can enhance the utilization of resources.

Although deploying DER close to the end-use sector tends to alleviate the original congestion problem, congestion may still exist if DG generation is not supervised properly. Recently, a study has been reported in the Pacific Northwest [28] indicating that a surplus of wind power has been noticed and may be shut down in its region. The same situation may occur in neighborhoods when the number of houses installed with solar units increases and when consumption is low. Congestion due to reverse power from solar panels in distribution grid has not yet been extensively studied. This paper proposes scheduling algorithms by analyzing the knapsack problem to efficiently select those solar units to be disconnected among households in the NAN. Wireless communications between smart meters (SMs) and the utility control center (UCC) is proposed to facilitate the congestion management.

3 SYSTEM MODELS

3.1 The Power System Model

In electric power systems, power flow analysis is essential to schedule and plan for the amount of power flows between two buses[3] of the interconnected system. Available Transfer Capability (ATC) of the transmission network is a measure of the transfer capability remaining in the physical transmission network for further commercial activity over and above already committed uses [29]. It has been a tool used for congestion management as well as for power marketers trading in the competitive electric market [30], [31]. ATC is computed as

$$ATC = TTC - TRM - ETC, \qquad (1)$$

where TTC (total transfer capability) is the maximum amount of power that can be transferred over the network in a reliable manner while satisfying all security constraints, i.e., thermal, voltage, and stability limits; transmission reliability margin (TRM) is the amount of transmission transfer capability necessary to ensure the network is secure under a reasonable range of uncertainties[4] in system conditions, and existing transmission commitments (ETC) include retail customer service and capacity benefit margin (CBM). CBM is the amount of transmission transfer capability reserved by load serving entities for generation reliability requirements [29]; it is reserved for emergency when power generation is insufficient in one area which needs to be supplied with purchased power from other regions [31]. ATC can be a very dynamic quantity for a specific time frame for a specific set of conditions. We use ATC in this paper as a key parameter to assess and mitigate the solar power surplus congestion problem.

---

3. A bus is electrically equivalent to a single point on a circuit, and it marks the location of one of two things: a generator that injects power, or a load that consumes power; it provides a reference point for measurements of voltage, current, and power flows [21].

4. Uncertainties of transfer capability that may occur during a power transfer are always considered in determining the ATC [32]; they may involve equipment failures, inaccurate network parameters, imprecise transfer capability computation, varying loads due to environment and weather conditions, and power cost change in the electricity market.
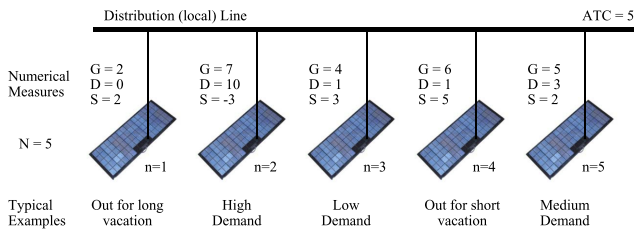
Fig. 1. An example of the systematic model.

Fig. 2. The grid-tie solar system mounted on rooftops.

We assume that ATC is calculated and available at the UCC periodically.[5] With such information, we can determine if the network at specific times is able to accommodate an aggregate of solar power surpluses. If not possible, a scheduling algorithm is required to disconnect some of solar units from the grid in order to maintain the system stability. Fig. 1 illustrates an example of *five* households with rooftop solar panels connected to the distribution line. Each household has its *energy profile* available that contains data for solar power generation (G), household power demand (D), and unused power flowing back to the grid (S). In this example, each household has a solar surplus except for household 2, which has a surplus value -3 because it is consuming more energy than it can produce. Household 2's demand 10 may be compensated by the existing power (i.e., ETC including CBM in (1)), by an aggregate of solar surpluses 12 produced from others, or by partial existing power and solar surpluses. In either case, power is drawn from the distribution line and household 2 has to remain on the grid. From the utility perspective, the residual surplus can be used for commercial trading while satisfying the ATC limit. Since the line capacity cannot hold the residual surpluses, disconnecting some of the solar units is one approach to congestion avoidance. A set of feasible solutions of allowing the solar units to remain connected with the grid include {1,3,5}, {1,4}, {3,4}, and {4,5}, where {.} represents a set of solar units. Despite the fact that choosing either of the combinations will not violate the ATC limit, we manage to maintain as large number of units as possible in selection so that the disconnection as well as reconnection can be minimized. Communications is required to perform the disconnection process. Efficient monitoring and congestion management can be provisioned via SMC (to be discussed in Section 3.2).

In this paper, we assume that the PV solar unit is a grid-tie system rather than an off-grid (stand-alone) system. In fact, the grid-tie unit is preferred not only because it has higher energy efficiency, but also because the off-grid unit requires a bank of batteries or capacitors equipped for storing power to supply on its own, thus resulting in an extra cost for households [33].

3.1.1 The Solar Array System

A grid-tie solar system mounted on rooftops or on ground without batteries backup is composed of four major

components: PV solar panels/array, direct current (DC) Disconnect, inverter, and alternating current (AC) Disconnect/AC breaker panel (ACDBP) [34]. As illustrated in Fig. 2, solar power is generated through the semiconductor cells of PV solar panels as a stream of direct current. The maximum amount of power that can be produced depends on various factors, such as sun intensity, temperature condition, and techniques implemented in the inverter, e.g., maximum power point tracking (MPPT) [35]. The DC power generated from the solar panels flows to the DC Disconnect (switch/breaker box). The DC flow can be prevented from entering the DC Disconnect during emergency or maintenance on the utility grid system. In a normal situation, the grid-tie inverter transforms the DC power collected from the DC Disconnect into alternating current power for most of residential and commercial uses. It produces power that meets the requirements of the utility grid so that the generated power is synchronized with the grid power before flowing into the grid. The ACDBP can also stop the current flow from entering the grid for emergency or maintenance purposes. Without the AC Disconnect, the consumer's load is also interrupted while the solar power is isolated from the grid [36].

There are essentially two ways to prevent the generated solar power from entering the grid: 1) Open the circuit between the solar panels and DC Disconnect, and 2) Open the circuit between the ACDBP and the grid. The former entirely isolates the generated power from the solar panels. The generated power may be grounded—this results in the lowest efficiency of energy use because households are unable to consume the energy. On the other hand, the latter[6] allows households to consume their solar power from the AC breaker panel through another dedicated line. Hence, this method is preferred despite the excess power also sent into the ground while unused. Once energy consumption rises and approaches the amount the solar panels generate, the ACDBP is reconnected to the grid and the grid power can be provisioned. Therefore, we consider the second case in this paper.

3.1.2 Congestion and Overload-Causes and Remedies

Unexpected power demand and renewable energy production can potentially instigate congestion in both transmission and distribution grids. From a consumer aspect, the variation and surge in loads are essentially attributed to consumers' needs and activities as well as environment and weather

---

5. ATC of power transfers among subnetworks of the entire interconnected transmission network cannot be evaluated in isolation; regional or wide-area coordination is necessary from all entities to gather and post sufficient information. Therefore, it is reasonable to assume that ATC has to be calculated in real time and available in order for network operators to be aware of the network congestion level.
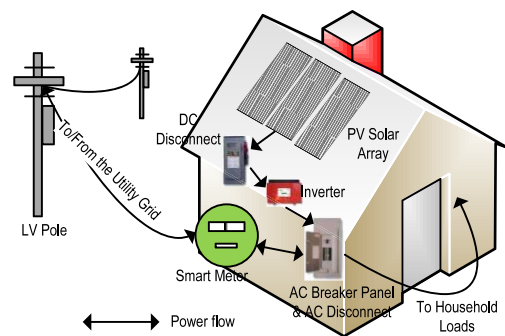
6. The SM stops measuring the solar power generation because the line between the SM and the ACDBP is disconnected.

conditions. The former is usually unpredictable where historical data of consumption are required to estimate the prospective loads in advance. The latter is supervised with the aid of weather forecast to match the correlated loads in specific regions and seasons. On the other hand, determination of transfer capability such as TTC and ATC (described in Section 3.1) in the interconnected grid is critical from a network perspective. Foreseeing the approximate amount of consumption without sufficient transfer capability calls for proper actions to avoid congestion. Therefore, demand response programs are applied to manipulate varying consumption such that consumers have a choice whether or not to consume energy based on the corresponding price signal received from utilities. The demand side management adopts peak shaving and valley filling strategies to reduce demand peak-to-average ratio, and at the same time to increase energy utilization.

Furthermore, solar power surpluses during renewable times can also overload the network when consumption is low and when the resources are limited, e.g., lack of energy storage, transfer capability, and transmission capacity. Several ways to tackle the issue may include

- *Sell excess power* to other regions in need or *maximize energy use* during renewables production. However, utilities may run out of capability to sell the surpluses when consumption is low or people not being home.
- *Shut down some power plants* such as fuel oil, natural gas, or even nuclear. Nevertheless, this may put the grid in danger due to the intermittency and variability of renewables generation. In addition, some generators cannot be turned back on within a short period of time.
- *Store surplus energy* in additional storage as much as possible for later use. Nonetheless, current energy storage is still expensive and inefficient.
- *Disconnect a number of solar units* from the grid.

In this paper, we adopt the last approach to mitigating solar surplus congestion in the distribution grid.

3.2 The Communications System Model

Communications in the legacy electric power system has been partially proprietary and based on simple protocols. In fact, no communications or simple communications is preferred in fault detection management [12]; shutdown is the quickest and safest way in the protection system. In order to enhance the network visibility for utility operators, integrating ICT and smart grid technologies is necessary for achieving effective distributed control and monitoring.

There are various choices of communications technologies for NAN and HAN [37]. We propose to implement wireless technologies either based on IEEE 802.11 WiFi [38] or IEEE 802.15.4g for NAN and IEEE 802.15.4 ZigBee [39] for HAN as part of SMC in the advanced meter infrastructure (AMI). IEEE 802.11 supports high data rate to relay an aggregate of data collected from SMs to the UCC. IEEE 802.15.4 provides reasonable data rates for small-size data packets with low power transmission, whereas IEEE 802.15.4g (smart grid utility network) tailors sub-GHz radio frequencies (RF) for better RF penetration and less interference. We follow the HAN design in [22] where each house is equipped with an
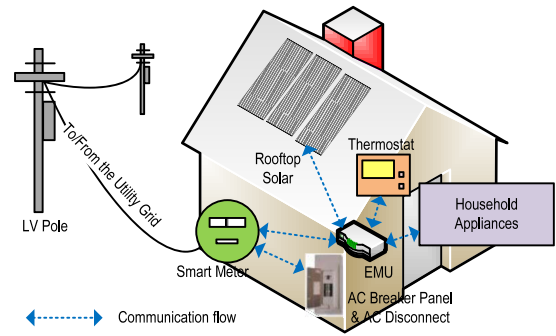

Fig. 3. Communications in HAN between SM and EMU as well as between EMU and solar unit, appliances, and thermostat.

energy management unit. In our proposed scheme (as shown in Fig. 3), the PV solar unit, household appliances, thermostat, and ACDBP, are physically connected with the SM. The SM has multiple built-in functionalities supporting different wired and wireless communications protocols of powerline communications (PLC) and RF technologies [40]. The EMU plays as an intermediate node (e.g., gateway) which coordinates households energy consumption and records solar generation. It also consults with the SM to determine if low energy cost can be obtained when grid power is needed. The SM also measures and records both solar power generation/surplus and households energy consumption. The measured data at the SM are transmitted to UCC via SMC. In Fig. 4, SMC in NAN consists of SMs, relay/aggregation nodes, and an UCC.

SMC is constructed as a wireless mesh network. Fig. 4 illustrates the case where a neighborhood is composed of 12 households and three relay nodes. Data packets containing energy profiles are periodically transmitted in uplink from the SMs, through relay nodes, and received at the UCC. Upon data reception, the UCC performs computation based on our proposed algorithms (to be discussed in Section 4) and sends the notification packets back to the SMs if their solar units need to be disconnected from the grid. For example, if the UCC determines that no power congestion is found in the network, no action is taken at the UCC. When unit disconnection is required, each SM associated with its corresponding solar unit to be disconnected receives notification from the UCC,[7] and sends a signal to ACDBP to disconnect its solar unit from the grid. Consequently, the SM stops measuring and transmitting data to the UCC.[8] Since the disconnection would not affect household consumption from the solar generation (as discussed in Section 3.1.1) for a period of time, data transmission between the SM and UCC is not required.[9] Once consumption arises or generation decreases and EMU is aware that grid power is needed while communicating with appliances and solar units, EMU notifies the SM of the event. The SM starts transmitting a request packet to the UCC to see whether

---

7. In the proposed mechanism, we minimize the number of disconnected units so that we may keep the number of notification packets in *downlink* as small as possible.
8. At the same time, we also minimize the number of data packets in *uplink* while households are disconnected from the power grid.
9. Disconnection makes the households equivalently operate in the islanded mode. Power is self-provisioned, therefore, no data transmission from the disconnected SMs during the disconnection period.
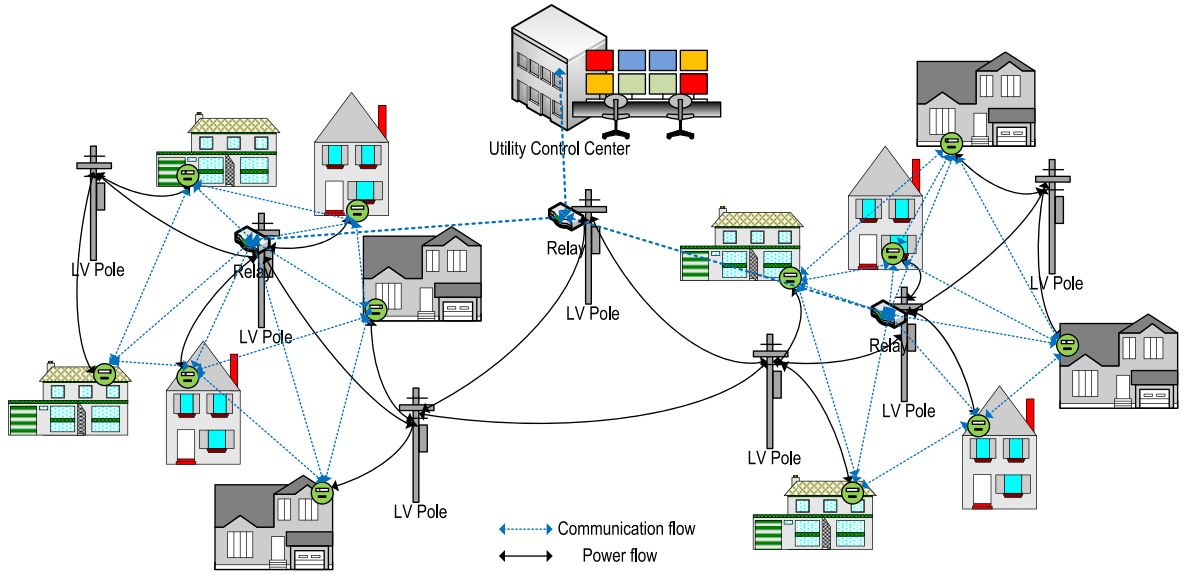
Fig. 4. Smart metering communications infrastructure in NAN.

reconnection can be done. The UCC replies with a price signal. If the household agrees to consume the grid power based on the time-of-use (TOU) price, the reconnection is granted. Otherwise, disconnection remains until congestion is relieved. For households which remain connected, the corresponding SMs periodically transmit data information to the UCC. The mechanism of the proposed system model is summarized in Algorithm 1.

Algorithm 1. The System Model for The Solar Unit Disconnection Process via SMC
Require: All units are connected to the grid.
Ensure: Periodic data transmission from SMs to UCC.
  while power congestion is discovered **do**
    if a unit has no surplus **then**
      Remain on the grid.
    else {a surplus exits}
      Disconnection is considered (discussed in Section 4)
      UCC signals units to be disconnected.
      The disconnected units stop transmitting data to UCC
      and stay in islanded and standby modes.
      Reconnection is granted from UCC when grid power
      is needed or congestion is removed.
    end if
  end while

4   PROBLEM FORMULATION

We consider N households which have PV solar units installed on rooftops or on ground in a neighborhood. Each household is denoted by $n, n = 1, 2, \ldots, N$, and the corresponding PV solar unit is denoted as x_n. Household n may (not) consume energy in Watt per hour (Wh) during solar power generation; the corresponding demand value is represented by a nonnegative integer and denoted by $P_{D,n} \in \mathbb{N}$. There is (not) power surplus from unit x_n when the generated power in Wh is more (less) than it is needed; the corresponding surplus value is an integer and denoted by $P_{S,n} \in \mathbb{Z}$. In the selection process, we only

consider $\widehat{N} = N \backslash M$ households being a positive integer in which M out of N households do not have surpluses (i.e., $P_{S,n \in M} \leq 0$) and have to remain on the grid. Finally, the capacity of the distribution line is a nonnegative integer and denoted by $P_{ATC} \in \mathbb{N}$. Table 1 defines a list of symbols we use in this paper.

4.1   Assumption
Without loss of generality, we have considered the following assumptions:

1. Sunlight is available most of the time during solar power production.
2. Variability of demands and surpluses is managed and controlled through EMU and SMs in HAN.
3. All solar units are grid-tie systems and no additional energy storage is available for households.
4. Households may continue to consume solar energy while solar units are disconnected from the grid.
5. The disconnection at the AC Disconnect can be done by the SM via communications.
6. Power loss and system constraints (e.g., real and reactive power in terms of voltage, frequency, and phase) are not considered.

TABLE 1
Symbols with Definitions Used for the Formulated Problem

Symbol	Definition	Symbol	Definition
N	A set of all households	x_n	PV solar system of household n
n	Household n	$\widehat{\mathbf{x}}$	A vector of PV solar systems ON/OFF status
$P_{D,n}$	Power demand variable of household n	U	Total number of connected units
$P_{S,n}$	Power surplus variable of household n	P_{ATC}	Power network available transfer capacity
η_n	Energy efficiency of household n	P_O	Power network overload indicator
η	Global energy efficiency	s	Split number (MNDS scheme)
M	A set of households which have no surpluses	P_E	Overflowed power (see Eq. (8))
$\widehat{N}$	A set of households which have surpluses	κ	Inspection range parameter for selection (RVS scheme)

4.2 Objective Function and Constraint

The solar power congestion issue in the distribution grid can be tackled as one type of knapsack problems. In our scenario, the solar units either remain *connected* on the grid or are *disconnected* from the grid. Therefore, we consider a 0/1 KP where $x_n = 0$ if unit n is scheduled to be *off* the grid and $x_n = 1$ to be *on* the grid. Therefore, the total number of connected units is calculated as

$$U = \sum_{n \in \widehat{N}} x_n, \quad x_n \in \{0, 1\}. \tag{2}$$

It is a binary (decision) integer programming problem. The objective is to maximize the number of connected units (equivalently to minimize the number of disconnected units) subject to a limited capacity that the network can accommodate the surpluses of connected units

$$
\begin{aligned}
\max \ & U \\
s.t. \ & \sum_{n \in \widehat{N}} P_{S,n} \cdot x_n \leq P_{ATC}, \quad x_n \in \{0, 1\}.
\end{aligned} \tag{3}
$$

From a power standpoint, maintaining a large number of connected units allows more households not only to use their solar power, but also to be able to sell the power surplus to the utility. From a communications perspective, data traffic congestion may be reduced owing to fewer packets sent out from the UCC for the disconnection process.

Meanwhile, we also aim to maximize the total power demand value while meeting the capacity requirement

$$
\begin{aligned}
\max \ & \sum_{n \in \widehat{N}} P_{D,n} \cdot x_n \\
s.t. \ & \sum_{n \in \widehat{N}} P_{S,n} \cdot x_n \leq P_{ATC}, \quad x_n \in \{0, 1\}.
\end{aligned} \tag{4}
$$

The strategy is to protect households with high energy efficiency from being disconnected. The efficiency of energy use of household n (η_n) is a nonnegative real number, and defined as the ratio of power demand to power surplus. Similarly, the global energy efficiency (η) is the ratio of cumulative power demands to cumulative power surpluses, i.e.,

$$
\begin{aligned}
\eta_n &= \frac{P_{D,n}}{P_{S,n}} \in \mathbb{R} | \eta_n \geq 0 \\
\eta &= \frac{\sum P_{D,n}}{\sum P_{S,n}} \in \mathbb{R} | \eta \geq 0, \quad n \in \widehat{N}.
\end{aligned} \tag{5}
$$

Taking energy efficiency into account will encourage the households with lower efficiency of energy use to utilize energy during solar power generation. Consequently, we will achieve the ultimate goal of having less power surpluses flowed to the grid, and more units connected to the grid.

4.3 Methods

SMC involves enormous data transmission between the UCC and SMs for various purposes, e.g., meter data collection, device control, and fault detection. The efficiency of computation at the UCC is critical to the system performance. When the UCC receives energy profiles from the SMs, it has to quickly figure out which ones among $\widehat{N}$ households should be disconnected from the grid once power congestion is detected. The number of households covered by a utility company can be as large as from thousands to hundreds of thousands. Using the brute-force approach to solving a KP problem would take $O(2^n)$ exponential time to obtain the result; the computation running time tends to escalate exponentially when the number of nodes increases. Since scalability is a main concern for both computation and communications, the network has to be divided into subnetworks to form a number of clusters. The decentralized scheme allows the UCC to manage and control data computation and data traffic more effectively.

The KP has been proven to be an NP-complete problem. Existing solutions to solve KPs include dynamic programming, backtracking, branch and bound, and greedy approaches. We intend to propose greedy algorithms to obtain a suboptimal solution that is good enough to avoid power congestion.

4.3.1 Dynamic Programming

Dynamic programming decomposes a KP problem into a number of local subproblems and computes optimal solutions of the subproblems to obtain a global optimal solution. Instead of finding all 2^n possible solutions exhaustively, DP looks at smaller capacities $c \leq C$ (from 1 to C) and determines which unit n (from 1 to N) can be included subject to the subcapacity limit while achieving the maximum demand value at each iteration. Therefore, DP requires a table (where DP trades space for time) to memoize the subsolutions. By looking up the table in a bottom-up manner, a global optimal solution can be obtained. The algorithm fills $(N+1)(C+1)$ entries in the table. Each entry requires 1 execution and we need N executions to trace the solution. The overall complexity is asymptotically reduced to $O(NC)$ [41], which is solvable in a polynomial time. Unfortunately, DP becomes prohibitive when the capacity C is too large, e.g., $>10^4$ in our problem. One way to reduce the size of the table is to find the greatest common divisor (GCD) among the surplus values and capacity, but the GCD usually equals 1 from a large set of values.

4.3.2 Greedy Strategy

Typically, a greedy algorithm can solve the KP in approximately $O(n)$ running time [41]. One greedy approach to our KP is to construct permutations by ordering the energy profiles collected at the UCC. Selecting the candidates among households can be based on the following three methods: the highest power demand first, the greatest power efficiency first, and the lowest power surplus first. The three strategies are described as follows:

1. *Nonincreasing power demand (NID)*. NID tends to maximize the total value of power demand disregarding the associated power surplus by adding demand values in descending order:

   $$P_{D,1} \geq P_{D,2} \geq \cdots \geq P_{D,n}, \quad n \in \widehat{N}.$$

   Because NID has a great potential to reach the capacity limit quickly, it has the worst performance in cumulative demands and U as compared to other schemes.

2. *Nonincreasing power efficiency (NIE)*. NIE aims to improve the NID scheme by considering surplus values as a complementary factor to balance the output of the system performance. NIE executes (5) and accumulates the demand values in descending order of energy efficiency:

$$\eta_1 \geq \eta_2 \cdots \geq \eta_n, \ n \in \widehat{N}.$$

Although a high power efficiency indicates efficient energy use, different combinations of demand and surplus values can have the same or similar ratios which are hard to differentiate; this is the key factor that prevents NIE from obtaining a large U. Overall, NIE achieves the highest total demand value among the three at the cost of a reduced U.

3. *Nondecreasing power surplus (NDS)*. NDS tends to pick as many units as possible while it accumulates surplus values in ascending order:

$$P_{S,1} \leq P_{S,2} \cdots \leq P_{S,n}, \ n \in \widehat{N}.$$

Therefore, the method achieves the largest U as compared to others. However, NDS disregards the corresponding demand values as opposed to NID. Our first proposed algorithm is to modify the NDS scheme by improving the overall energy efficiency.

4.4 The Proposed Algorithms

While introducing the ordering strategy for unit selection, we develop two algorithms by adopting the NDS scheme to fulfill the first optimization problem, i.e., (3). Note that it is reasonable to select a unit beginning with the smallest surplus because its energy efficiency is likely high; however, in the case where a unit with a small surplus is due to a small amount of generation, its energy efficiency can be low if the demand is small. Moreover, we keep units which have small surpluses connected to the grid in order to avoid frequent disconnection and reconnection. This is because the corresponding demands can fluctuate such that surpluses may no longer exist and yet the grid power is required. Therefore, for the first proposed scheme, we combine NDS with NIE to enhance the overall energy efficiency and demand, i.e., (4). For the second proposed scheme, we apply NDS backwards with NIE to get rid of units (to be disconnected) which do not meet our design criteria. Meanwhile, the capacity constraint must hold.

4.4.1 Modified NDS (MNDS)

Methodology. We assume that data information about solar power demands and surpluses of N households have been collected from the SMs and available at the UCC. We only consider $\widehat{N}$ units when other M units do not have surpluses available. No units are disconnected while the network is not overloaded. The overload status of the network is discovered by subtracting the capacity limit by the total surplus of $\widehat{N}$ units

$$P_O = \sum_{n \in \widehat{N}} P_{S,n} - P_{ATC}. \tag{6}$$

When overload is detected (i.e., $P_O > 0$), the NDS scheme is performed (see Lines 7-16 in Algorithm 2). Units are selected based on their surpluses in ascending order. After some
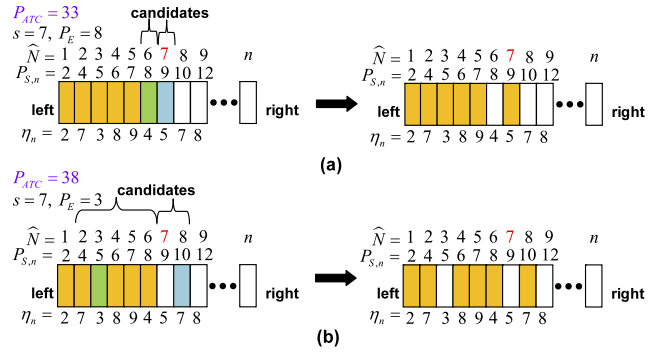

Fig. 5. An illustration of the MNDS algorithm. Two situations during the substitution are shown, where (a) depicts only one candidate found in $\widehat{x}_l$ and $\widehat{x}_r$, respectively, and (b) demonstrates multiple candidates found in $\widehat{x}_l$ and $\widehat{x}_r$, respectively.

iterations, the algorithm will stop at iteration i when an overload of the capacity is found, i.e.,

$$\sum_{n=1}^{s-1} P_{S,n} \leq P_{ATC} \text{ and } \sum_{n=1}^{s} P_{S,n} > P_{ATC}, \ n \in \widehat{N}.$$

Note that $P_{S,s}$ cannot be added because the capacity constraint will be violated. We assign unit s to be the *split unit*, which constitutes the solution vector $\widehat{x}$ with $\widehat{x}_n = 1$ for $n = 1, 2, \ldots, s-1$ and $\widehat{x}_n = 0$ for $n = s, s+1, \ldots, \widehat{N}$, i.e.,

$$\widehat{x} = [\widehat{x}_1 \ \widehat{x}_2 \ \ldots \ \widehat{x}_{s-1} \ \widehat{x}_s \ \widehat{x}_{s+1} \ \ldots \ \widehat{x}_{\widehat{N}}]$$
$$= [\underbrace{1 \ \ 1 \ \ \ldots \ \ 1}_{\widehat{x}_l} \ \ \underbrace{0 \ \ 0 \ \ \ldots \ \ 0}_{\widehat{x}_r}]. \tag{7}$$

$P_{S,s}$ is defined as the *split surplus value*. Unlike the original NDS scheme, MNDS tries to further improve the overall energy efficiency from what NDS can achieve while maintaining U, i.e., $s-1$ units. In order to do this, we calculate the overflowed power when the split surplus value is added

$$P_E = \sum_{n=1}^{s} P_{S,n} - P_{ATC}, \quad n \in \widehat{N}. \tag{8}$$

With the knowledge of P_E, which is incorporated into the two conditions (Lines 21 and 25) specified in Algorithm 2, we may determine the number of candidate units in $\widehat{x}_l$ and $\widehat{x}_r$ (see (7)) to be considered for a one-to-one substitution. Fig. 5 illustrates the surplus values of $\widehat{N}$ units sorted in ascending order from left to right, and the corresponding energy efficiency values for the comparison purpose.

Algorithm 2. Modified NDS
1: Determine if the capacity is overloaded (Eq. 6)
2: **if** $P_O \leq 0$ **then**
3:     Disconnect none
4: **else**
5:     Sort surpluses in *ascending* order
6:     **if** $P_{ATC} >$ the min surplus among $\widehat{N}$ units **then**
7:         $c = P_{ATC}$
8:         **for** $i = 1$ **to** $\widehat{N}$ **do**
9:             **if** $P_{S,i} \leq c$ **then**
10:               $c = c - P_{S,i}$ {Keep unit i ON}
11:             **else**

12:          No more units can be accommodated
13:          $s = i$
14:          Break
15:       end if
16:    end for
17:    $w = s - 1$
18:    Calculate the overflowed power P_E (Eq. 8)
19:    for $j = 1$ to w do
20:       Find candidate(s) in $\widehat{\mathbf{x}}_l$
21:       if $P_E \leq P_{S,j}$ then
22:          One in $\widehat{\mathbf{x}}_l$ among units j-$(s-1)$ with min η is
              the candidate η_l of unit l
23:          for $k = s + 1$ to $\widehat{N}$ do
24:             Find candidate(s) in $\widehat{\mathbf{x}}_r$
25:             if $P_{S,k} - P_{S,s} > P_{S,l} - P_E$ then
26:                One in $\widehat{\mathbf{x}}_r$ among units s-$(k-1)$ with max η
                   is the candidate η_r of unit r
27:                if $\eta_l < \eta_r$ then
28:                   Unit l is substituted by unit r
29:                end if{Nothing changed otherwise}
30:                Break
31:             end if
32:          end for
33:          Break
34:       end if
35:    end for
36:    end if{Disconnect all otherwise}
37: end if

Considering $P_{ATC} = 33$ as shown in Fig. 5a, unit 7 is found to be the split unit (whose surplus value is 9) while the first six units have an aggregate of surplus values of *32*. Adding the split surplus value would make the total *41* and result in overload. While knowing $P_E = 8$ derived from (8), unit 6 whose surplus value is 8 is determined to be the only one candidate in $\widehat{\mathbf{x}}_l$ (Lines 21-22). Subsequently, the outcome of searching for candidates in $\widehat{\mathbf{x}}_r$ is unit 7 only (Lines 25-26). As a result, unit 6 is removed from the list and unit 7 which has higher energy efficiency is added without exceeding the capacity limit, i.e., $\sum_{n=1}^{5} P_{S,n} + P_{S,7} = 33 \leq P_{ATC}$.

In another situation where more than one units found in $\widehat{\mathbf{x}}_l$ and $\widehat{\mathbf{x}}_r$, we assume $P_{ATC} = 38$ as shown in Fig. 5b. The split unit is unit 7 again and $P_E = 3$ is derived, implying that any surplus values larger than or equal to 3 in $\widehat{\mathbf{x}}_l$ are qualified for substitution, i.e., units *2-6*. While unit 3 whose surplus value is 5 happens to have the lowest efficiency value among others, we intend to find the units in $\widehat{\mathbf{x}}_r$ that satisfy the requirement (line 25) by subtracting P_E by $P_{S,3}$ (i.e., $5 - 3 = 2$) and by subtracting $P_{S,7}$ by $P_{S,9}$ (i.e., $12 - 9 = 3$). The outcome shows the candidates in $\widehat{\mathbf{x}}_r$ to be units 7 and 8. As a result, unit 3 is substituted by unit 8 whose energy efficiency is higher than that of units 7 and 3, without exceeding the capacity limit, i.e., $\sum_{n=1}^{2} P_{S,n} + \sum_{n=4}^{6} P_{S,n} + P_{S,8} = 37 \leq P_{ATC}$. While the one-to-one substitution can preserve as many units as NDS can, MNDS outperforms NDS in greater energy efficiency once an available substitute is found.

Complexity. The MNDS scheme inherits the property of the sorting algorithm (Line 5) which approximately takes $n \log(n)$ executions in the average and worst cases. Accumulation of surplus values may take $(1+1) + [n(1+1)+1]$
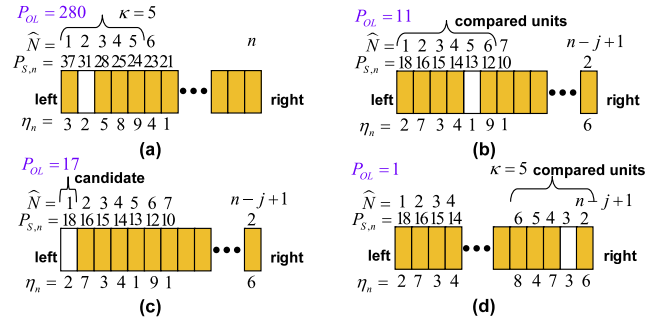

Fig. 6. An illustration of the RVS algorithm. Four situations during the deselection process are shown, where (a) depicts the first five units being compared during the first $j - 1$ iterations, while (b), (c), and (d) demonstrate the last iteration j being performed; (b) depicts a comparison among the first six units; (c) depicts the first unit being deselected when it is the only one that satisfies the condition; and (d) depicts a comparison among the last five units.

executions (Lines 6-7 and 8-16, correspondingly) while determining the overload status (Lines 1-2) and calculating P_E (Lines 17-18) can take $n + 1$ executions each. The main feature of MNDS is searching for candidates in both $\widehat{\mathbf{x}}_l$ (Lines 19-22) and $\widehat{\mathbf{x}}_r$ (Lines 23-26) that can take n executions each, as well as comparing the final candidate in $\widehat{\mathbf{x}}_l$ with the final candidate in $\widehat{\mathbf{x}}_r$ that requires 2 executions (Lines 27-28). Therefore, the overall complexity of MNDS is asymptotically reduced to $O(n \log(n))$.

4.4.2 Reverse Selection (RVS)
Methodology. We further propose a reverse method to deselect units to be disconnected from the grid instead of selecting units to be connected in the previous methods. The RVS scheme is preferred when the number of disconnected units is less than $\widehat{N}/2$. In order to do this, we will sort the energy profiles in descending order of surplus values from left to right, as shown in Fig. 6. The RVS scheme deselects units with lower energy efficiencies among others according to the requirements constituted in Algorithm 3, where two conditions are considered: iterations prior to the last iteration (Line 23), and the last iteration (Lines 11, 17, 20).

Algorithm 3. Reverse Selection Algorithm
1: if $P_{ATC} <$ the min surplus among $\widehat{N}$ units then
2:    Disconnect all units
3: else
4:    Sort surpluses in *descending* order
5:    Pick κ
6:    for $j = 1$ to $\widehat{N}$ do
7:       if $P_O < P_{S,\widehat{N}}$ then
8:          if $P_O \leq 0$ then
9:             Break {Disconnect none}
10:         else
11:            Disconnect one with min η among the last κ units
               (see Fig. 6d)
12:            Break
13:         end if
14:      else
15:         if $P_O \leq P_{S,1}$ then
16:            if $P_O > P_{S,2}$ then
17:               Disconnect the *first* unit (see Fig. 6c)
18:               Break

19:      **else** {see Fig. 6b}
20:         Disconnect one with min η among units 1-$(i-1)$ such that $P_O > P_{S,i}$
21:         Break
22:      **end if**
23:   **else** {Next round is required; see Fig. 6a}
24:      Disconnect one with min η among units 1-κ
25:   **end if**
26:   **end if**
27:   **end for**
28: **end if**

Similarly, we assume that data information about demands and surpluses are received at the UCC. We again identify whether the network is overloaded by executing (6). If overload is observed (i.e., $P_O > 0$), the deselection process begins. The permutation is constructed by sorting the surplus values of units in descending order that is contrary to NDS and MNDS. When multiple iterations are required to deselect units during the process (i.e., when the updated overload value is larger than the greatest surplus value, see Lines 15 and 23), we inspect an arbitrary number κ of units from the first unit and select one unit that has the lowest energy efficiency (Line 24). The parameter κ is an adjustable number which defines the inspection range in the RVS scheme, where $\kappa = 1, 2, \ldots, \widehat{N}$. Considering $P_O = 280$ shown in Fig. 6a, one iteration of deselecting a unit is not enough to fulfill the capacity constraint. In this situation, we compare the first five surplus values of units and deselect unit 2 in order to maintain a high energy efficiency. Notably, picking a large κ may increase the overall energy efficiency and demand at the cost of a smaller U as compared to NDS and MNDS; the outcome of RVS would approach that of NIE. Also note that when $\kappa = 0$, the outcome of RVS would be identical to that of NDS in reverse. The recursion continues until the residual overload at iteration j is found either larger than or smaller than the surplus value of the last unit, i.e., unit $\widehat{N} - j + 1$. Both cases indicate one more unit to be deselected. In the former case (Lines 15-22), the overload value is compared with the surpluses starting from the first unit until it is found greater than the ith surplus. Since the first $i - 1$ surpluses are larger than the overload value, one of them with the least energy efficiency is chosen for disconnection. For examples, assuming $P_O = 11$ as shown in Fig. 6b, those before unit 7 (i.e., units *1-6*) will require a comparison of their energy efficiencies. As a result, unit 5 is deselected. Furthermore, Fig. 6c shows a particular situation where $P_O = 17$; unit 1 with surplus value being larger than the overload value is directly deselected without a comparison. On the other hand, the latter case (Lines 11-12) applies the same method for the recursive iterations such that the last κ units are compared, and one of them with the minimum energy efficiency is chosen for disconnection. Fig. 6d considers $P_O = 1$, where unit $n - j$ whose surplus value is 3 is deselected among the last five units.

Complexity. The RVS algorithm also involves the sorting process which takes $n \log(n) + 1 + 1$ executions (Lines 1-5). Since the complexity of RVS is dominated by the first $j - 1$ iterations, we can neglect the complexity of the last iteration j, i.e., $max\{1, 1 + \kappa, 1 + 1, 1 + i - 1\}$ corresponding to Lines 8, 11, 16, 17, and 20, respectively. In the worst case, the first $j - 1$

iterations can take approximately $n(1 + 1 + \kappa) \sim n^2$ executions if $\kappa = n$ (Line 24). However, the purpose of RVS is to enhance the overall efficiency while preserving as large U as possible; κ is chosen to be small so that the overall complexity of RVS can still be asymptotically reduced to $O(n \log(n))$.

5 SIMULATION RESULTS AND ANALYSIS

Our simulations are twofold: the first set is undertaken to demonstrate the viability of the selection algorithms (NID, NIE, NDS, MNDS, and RVS), whereas the second set is conducted to examine the upstream data traffic in a SMC network.

5.1 Simulation for the Selection Algorithms

The first simulation represents a special case assuming that power surplus exists from each household (i.e., all N units are considered in the selection process; $M = 0$), whereas the second simulation shows a general situation in which some households consuming more power than they produce must remain on the grid, i.e., only $\widehat{N}$ units are taken into account; $M > 0$. For both simulations, we set $P_{ATC} = 30,000$ and $\kappa = 5$.

In the first simulation, $N = 50$ is set for scenarios (a)-(e), (g), and (h), in Table 2. Note that both scenarios (e) and (f) are the same (i.e., sharing identical probability distributions and parameters); hence, scenario (e) with $N = 50$ and scenario (f) with $N = 500$ are set to observe the effect of N becoming large. The power demand value (P_D) and power surplus value (P_S) are generated according to uniform distribution (UD) denoted by $\mathcal{U}(min,max)$ and folded-Gaussian distribution (FGD)[10] denoted by $\mathcal{FG}(\mu, \sigma^2)$. P_D and P_S are discrete random variables with probability mass functions (PMFs) $f_D(P_D; \mu_D, \sigma_D)$ and $f_S(P_S; \mu_S, \sigma_S)$, respectively. Different parameters are designed in *eight* scenarios to elicit how the variations can affect the selection schemes. Fig. 7 explicitly illustrates various PMFs and Table 2 summarizes the outcomes correspondingly. One thousand experiments are run to average the results for each scenario.

In each scenario, different widths of PMFs (determined by σ_D and σ_S) and (non)overlap between the two PMFs (determined by μ_D and μ_S) are presented. An ideal situation in which the efficiency of energy use is high for each household ($\eta \gg 1$) is mostly found in Figs. 7a, 7c, and 7d, whereas the opposite ($\eta \ll 1$) in Fig. 7h. Figs. 7e and 7f consider a full overlap between the two PMFs while others test on partial overlaps. From Table 2, we can determine when the NDS, MNDS, and RVS schemes are able to outperform NIE with respect to U. We first observe that the NID scheme has the worst performance in all cases; this is because NID disregards surplus values in favor of high demand values while accumulating demand values in descending order. Second, the NIE scheme obtains the highest cumulative demand values most of the time and can achieve as large U as NDS can in some conditions (e.g., Tables 2a, 2c, and 2h); however, NIE cannot always achieve a large U due to the nonincreasing accumulation of energy efficiency, which is directly proportional to demand values,

---

10. FGD is derived from the Gaussian distribution $\mathcal{N}(\mu, \sigma^2)$ by taking the absolute values of all negative real numbers and rounding them to the nearest integers. In other words, if X is a discrete Gaussian random variable with mean μ and variance σ^2, $D = |X|$ is a discrete folded Gaussian random variable that has a folded Gaussian distribution.

TABLE 2
The Outcomes of Algorithms Applied to Different Scenarios in Fig. 7 Correspondingly

$M = 0$

(a) Small σ_D and σ_S $(D > S)$, N=50

scheme	demand	surplus	η	$\bar{\eta}$	U	$\bar{U}$	demand	surplus	η	$\bar{\eta}$	U	$\bar{U}$
	UD						FGD					
NID	182892	29771	6.14	0.96	40	0.95	131245	29849	4.40	0.89	31	0.86
NIE	188472	29578	6.37	1	42	1	145415	29507	4.93	1	36	1
NDS	187470	29539	6.35	0.99	42	1	143557	29393	4.88	0.99	36	1
MNDS	188141	29580	6.36	0.99	42	1	144845	29517	4.91	0.99	36	1
RVS	188533	29770	6.33	0.99	42	1	145389	29608	4.91	0.99	36	1

(b) Large σ_D and σ_S, N=50

scheme	demand	surplus	η	$\bar{\eta}$	U	$\bar{U}$	demand	surplus	η	$\bar{\eta}$	U	$\bar{U}$
	UD						FGD					
NID	106403	29760	3.58	0.86	18	0.72	105357	29898	3.52	0.84	14	0.56
NIE	123358	29513	4.18	1	24	0.96	124362	29634	4.20	1	22	0.88
NDS	114393	29097	3.93	0.94	25	1	103848	28779	3.61	0.86	25	1
MNDS	117908	29389	4.01	0.96	25	1	110361	29501	3.74	0.89	25	1
RVS	120681	29623	4.07	0.97	25	1	115945	29374	3.95	0.94	25	1

(c) Small σ_D and large σ_S, N=50

scheme	demand	surplus	η	$\bar{\eta}$	U	$\bar{U}$	demand	surplus	η	$\bar{\eta}$	U	$\bar{U}$
	UD						FGD					
NID	84617	29767	2.84	0.72	18	0.72	63426	29887	2.12	0.60	14	0.56
NIE	114893	29226	3.93	1	25	1	102382	29006	3.53	1	25	1
NDS	114405	29160	3.92	0.99	25	1	101384	28824	3.52	0.99	25	1
MNDS	114874	29241	3.93	0.99	25	1	102292	29045	3.52	0.99	25	1
RVS	114951	29453	3.90	0.99	25	1	102395	29046	3.53	1	25	1

(d) Large σ_D and small σ_S, N=50

scheme	demand	surplus	η	$\bar{\eta}$	U	$\bar{U}$	demand	surplus	η	$\bar{\eta}$	U	$\bar{U}$
	UD						FGD					
NID	198752	29781	6.67	0.99	40	0.95	175315	29852	5.87	0.98	31	0.86
NIE	200044	29724	6.73	1	41	0.98	177548	29775	5.96	1	33	0.92
NDS	187629	29546	6.35	0.94	42	1	145835	29379	4.96	0.83	36	1
MNDS	191528	29640	6.46	0.96	42	1	153743	29690	5.18	0.87	36	1
RVS	194631	29812	6.53	0.97	42	1	161544	29764	5.43	0.91	36	1

(e) Same PMFs and $\sigma_D = \sigma_S$, N=50

scheme	demand	surplus	η	$\bar{\eta}$	U	$\bar{U}$	demand	surplus	η	$\bar{\eta}$	U	$\bar{U}$
	UD						FGD					
NID	43658	29573	1.48	0.84	12	0.67	72087	29891	2.41	0.83	13	0.54
NIE	51774	29445	1.76	1	17	0.94	86010	29615	2.90	1	21	0.88
NDS	46053	28925	1.59	0.91	18	1	70843	28752	2.46	0.85	24	1
MNDS	48246	29272	1.65	0.94	18	1	75548	29467	2.56	0.88	24	1
RVS	49946	29581	1.69	0.96	18	1	79741	29323	2.72	0.94	24	1

(f) Same PMFs and $\sigma_D = \sigma_S$, N=500

scheme	demand	surplus	η	$\bar{\eta}$	U	$\bar{U}$	demand	surplus	η	$\bar{\eta}$	U	$\bar{U}$
	UD						FGD					
NID	48344	29616	1.63	0.56	12	0.44	123999	29991	4.1345	0.4337	16	0.21
NIE	86110	29589	2.91	1	25	0.93	285445	29940	9.5339	1.0000	66	0.84
NDS	67820	29389	2.31	0.79	27	1	229768	29625	7.7559	0.8135	79	1
MNDS	70473	29486	2.39	0.82	27	1	236359	29846	7.9193	0.8306	79	1
RVS	73382	29617	2.48	0.85	27	1	245104	29831	8.2164	0.8618	79	1

(g) Different PMFs and $\sigma_D = \sigma_S$, N=50

scheme	demand	surplus	η	η	U	$\bar{U}$	demand	surplus	η	η	U	$\bar{U}$
	UD	FGD					FGD	UD				
NID	42545	29832	1.43	0.82	16	0.67	46723	29596	1.58	0.92	15	0.71
NIE	51300	29428	1.74	1	23	0.96	50450	29545	1.71	1	18	0.86
NDS	47948	29026	1.65	0.95	24	1	41187	29088	1.42	0.83	21	1
MNDS	49360	29310	1.68	0.97	24	1	44015	29530	1.49	0.87	21	1
RVS	50426	29494	1.71	0.98	24	1	46098	29671	1.55	0.91	20	0.95

(h) Small σ_D and σ_S $(S > D)$, N=50

scheme	demand	surplus	η	η	U	$\bar{U}$	demand	surplus	η	η	U	$\bar{U}$
	UD						FGD					
NID	5877	27342	0.21	0.98	6	0.86	11627	28769	0.4042	0.97	7	0.78
NIE	6320	27415	0.22	1	7	1	12058	28893	0.4173	1	8	0.89
NDS	5245	28553	0.18	0.84	7	1	8628	28343	0.3044	0.73	9	1
MNDS	5652	28741	0.20	0.89	7	1	9863	28799	0.3425	0.82	9	1
RVS	6182	29295	0.21	0.96	7	1	11152	28855	0.3865	0.93	8	0.89

$M > 0$

(i) Small σ_D and large σ_S | Large σ_D and small σ_S, N=100

scheme	demand	surplus	η	η	U	$\bar{U}$	demand	surplus	η	η	U	$\bar{U}$
	UD	FGD					FGD	UD				
NID	114609	29946	3.83	0.83	48	0.73	219744	29864	7.36	0.99	82	0.93
NIE	135852	29616	4.59	1	64	0.97	221650	29724	7.46	1	85	0.97
NDS	131288	29276	4.48	0.98	66	1	205716	29129	7.06	0.95	88	1
MNDS	132806	29468	4.51	0.98	66	1	209898	29534	7.11	0.95	88	1
RVS	134936	29648	4.55	0.99	65	0.98	215536	29640	7.27	0.98	88	1

(j) Large σ_D and σ_S, N=100

scheme	demand	surplus	η	η	U	$\bar{U}$	demand	surplus	η	η	U	$\bar{U}$
	UD						FGD					
NID	332154	29896	11.11	0.95	72	0.88	428280	29753	14.39	0.98	77	0.89
NIE	345234	29573	11.67	1	79	0.96	437144	29388	14.87	1	83	0.95
NDS	328022	28875	11.36	0.97	82	1	409186	27736	14.75	0.99	87	1
MNDS	332617	29272	11.36	0.97	82	1	416713	29076	14.33	0.96	87	1
RVS	338486	29516	11.47	0.98	82	1	425492	28986	14.68	0.99	87	1

Note that $\bar{\eta}$ is the ratio of the energy efficiency of schemes (NID, NDS, MNDS, RVS) to that of NIE, and $\bar{U}$ is the ratio of the total number of connected units achieved in schemes (NID, NIE, MNDS, RVS) to that in NDS.

similar to NID. Examples can be found in Tables 2b, 2d, 2e, 2f, and 2g; larger σ_D and σ_S likely yield more combinations having the same or similar energy efficiency values.

Furthermore, we set $N = 100$ in the second simulation where only units with surpluses are considered for selection. Two scenarios are shown in Figs. 7i and 7j and Tables 2i and 2j, and similar outcomes are also achieved. From the set of these two simulations, we observe that a number of conditional factors must be satisfied in order for the proposed schemes to outperform NIE with respect to U:

1. both σ_D and σ_S are large,
2. $\sigma_D \geq \sigma_S$,
3. σ_S cannot be too small,
4. there is a partial overlap between $f_D(P_D)$ and $f_S(P_S)$, and
5. κ must be small enough.

5.2 Simulation for Uplink Data Traffic via SMC

The environment for simulating the SMC network is developed under OPNET Modeler. We construct the SMC network consisting of one UCC and 50 SMs randomly placed in a 500×500 square meters area (as shown in Fig. 8a) and

adopt the IEEE 802.15.4 standard protocol for its wireless communications infrastructure; a ZigBee coordinator (used for UCC) and ZigBee routers (used for SMs) with full functionalities are selected in order to form a mesh topology. The frequency band of 2.4 GHz is chosen to support a data rate of up to 250 kb/s depending on the distance between the devices up to 100 meters, as described in [39]. In the SMC network (presented in Section 3.2), each SM periodically transmits a data packet with its energy profile information to the UCC. The UCC has no packets to send back to SMs until notification packets for disconnection are required. Since most of the data packets are involved in the upstream of the SMC, we will only consider the upstream data traffic in this paper during the selection process.

Three scenarios are developed in the simulation: the first scenario represents a default situation where periodic data transmission from SMs to UCC always takes place even if some SMs are disconnected from the grid; the second scenario assumes 25 SMs are called to disconnect from the grid (therefore, stop data transmission), and the disconnected SMs are assumed to be dispersed or balanced throughout the topology (shown in Fig. 8b); the third scenario follows the second scenario except that the

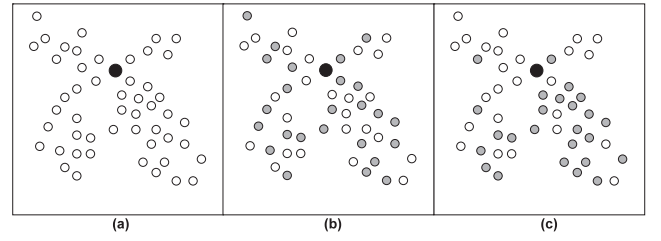Fig. 7. PMFs of demand and surplus corresponding to the scenarios in Table 2.

Fig. 8. The network topology in which the dark circle represents UCC whereas white/gray circles represent the connected/disconnected SMs.

approximately 1,200 second. From the simulation results as shown in Fig. 9, the total data traffic is reduced by approximately 50 percent whereas E2E delay is reduced by 4-8 percent; this is because the proposed algorithm halts the data transmission from the disconnected SMs during the disconnection period. Note that the location of disconnected SMs based on the selection process may affect the performance of data traffic and E2E delay. As observed from Fig. 9, the topology of disconnected SMs located in a concentrated region involves more data traffic (due to extra control bits) and larger E2E delay than that located in a dispersed manner. A further investigation on this outcome is required for the future work.

6 CONCLUSION AND FUTURE WORK

In this paper, we have investigated congestion in the electric power system. Congestion can occur in a traditional way due to variability of demands and intermittency of renewable energy when network resources are limited. Similarly, congestion is foreseen to exist in the distribution grid when the number of solar units in neighborhoods increases and when energy consumption is low. We formulate the solar surplus congestion in the distribution grid as one type of 0/1 knapsack problems and solve it with greedy strategies. We achieve our objectives by maximizing the number of connected units on the grid as well as improving cumulative demand values subject to the power capacity constraint. Computation time of the selection algorithms as well as data traffic loads in the smart metering communications is taken into consideration. We have shown via extensive simulations that the proposed algorithms for disconnecting solar units during the selection process have achieved the objectives. Our models for (dis/re)connection minimize computation time at the utility control center. The upstream data traffic via smart metering communications and corresponding end-to-end delay are also reduced based on our

disconnected SMs are concentrated mostly in one area (shown in Fig. 8c). For each scenario, acknowledgment for data reception is activated and different sizes for data packets transmitted from SMs to the UCC are tested: 500 b, 1 kb, and 2 kb. Furthermore, each SM transmits a data packet to the UCC every 5 seconds and the simulation time lasts for an hour. A notification of disconnection is taken place at
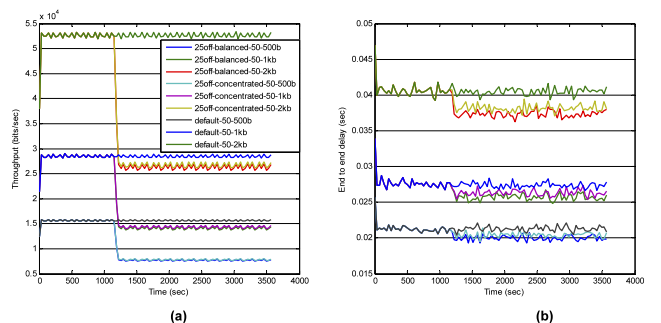

Fig. 9. Involved data traffic (a) and global end-to-end delay (b) between the UCC and SMs.

simulation results. Our proposal benefits utilities in both economic and technical terms.

For the future work, we will investigate the packet loss due to wireless impairments and the effect of bursty traffic on system performance. Furthermore, the proposed algorithms for solar disconnection due to varying demands and surpluses may yield different selection solutions. We will take the differences into account while they can have potentials to alter the network topology at different periods; meanwhile, fairness in selection should also be determined. Moreover, combining other distributed generation such as wind and microCHP with the PV solar system will also be considered in our future research endeavor.

REFERENCES

[1] C. Singh and A. Sprintson, "Reliability Assurance of Cyber-Physical Power Systems," *Proc. IEEE Power and Energy Soc. General Meeting*, pp. 1-6, July 2010.

[2] D.E. Bakken, R.E. Schantz, and R.D. Tucker, "Smart Grid Communications: QoS Stovepipes or QoS Interoperability," *Proc. Grid-Interop Conf.*, Nov. 2009.

[3] M. Rosenfield, "The Smart Grid and Key Research Technical Challenges," *Proc. Symp. VLSI Technology (VLSIT)*, pp. 3-8, June 2010.

[4] M. Sooriyabandara and J. Ekanayake, "Smart Grid - Technologies for Its Realisation," *Proc. IEEE Int'l Conf. Sustainable Energy Technologies (ICSET)*, pp. 1-4, Dec. 2010.

[5] T. Overman and R. Sackman, "High Assurance Smart Grid: Smart Grid Control Systems Communications Architecture," *Proc. First IEEE Int'l Conf. Smart Grid Comm.*, pp. 19-24, Oct. 2010.

[6] A. Kwasinski, "Implication of Smart-Grids Development for Communication Systems in Normal Operation and During Disasters," *Proc. 32nd Int'l Telecomm. Energy Conf. (INTELEC)*, pp. 1-8, June 2010.

[7] U.S. Energy Information Administration, Ann. Energy Rev. 2009, http://www.eia.gov/totalenergy/data/annual/pdf/aer.pdf, Aug. 2010.

[8] *U.S. Department of Energy*, Nat'l Electric Transmission Congestion Study, http://congestion09.anl.gov/documents/docs/Congestion_Study_2009.pdf, Dec. 2009.

[9] S. Güner and B. Bilir, "Analysis of Transmission Congestion Using Power-Flow Solutions," *Proc. Fifth IASME/WSEAS Int'l Conf. Energy and Environment*, pp. 330-333, 2010.

[10] S. Dehghan, M. Moradi, and A. Mirzaei, "Improving Congestion Relief Management as Ancillary Service in Operation Planning Phase with Demand Side's Presence," *Canadian J. Electrical and Electronics Eng.*, vol. 2, no. 5, pp. 145-152, May 2011.

[11] N. Hatziargyriou, H. Asano, R. Iravani, and C. Marnay, "Micro-grids," *IEEE Power and Energy Magazine*, vol. 5, no. 4, pp. 78-94, July/Aug. 2007.

[12] R. Lasseter, "CERTS Microgrid," *Proc. IEEE Int'l Conf. System of Systems Eng. (SoSE)*, pp. 1-5, Apr. 2007.

[13] A. Dobakhshari, S. Azizi, and A. Ranjbar, "Control of Microgrids: Aspects and Prospects," *Proc. IEEE Int'l Conf. Networking, Sensing and Control (ICNSC)*, pp. 38-43, Apr. 2011.

[14] C. Marnay, H. Asano, S. Papathanassiou, and G. Strbac, "Policy-making for Microgrids," *IEEE Power and Energy Magazine*, vol. 6, no. 3, pp. 66-77, May/June 2008.

[15] K. De Brabandere, K. Vanthournout, J. Driesen, G. Deconinck, and R. Belmans, "Control of Microgrids," *Proc. IEEE Power Eng. Soc. General Meeting*, pp. 1-7, June 2007.

[16] J. Liu, M. Salama, and R. Mansour, "Identify the Impact of Distributed Resources on Congestion Management," *IEEE Trans. Power Delivery*, vol. 20, no. 3, pp. 1998-2005, July 2005.

[17] A. Ipakchi and F. Albuyeh, "Grid of the Future," *IEEE Power and Energy Magazine*, vol. 7, no. 2, pp. 52-62, Mar./Apr. 2009.

[18] A. Saini and A. Saxena, "Optimal Power Flow Based Congestion Management Methods for Competitive Electricity Markets," *Int'l J. Computer and Electrical Eng.*, vol. 2, no. 1, pp. 73-80, Feb. 2010.

[19] B. Liu, J. Kang, N. Jiang, and Y. Jing, "Cost Control of the Transmission Congestion Management in Electricity Systems Based on Ant Colony Algorithm," *Energy and Power Eng.*, vol. 3, no. 1, pp. 17-23, Feb. 2011.

[20] L.L. Grigsby, *Power Systems*, ser. The Electrical Engineering Handbook, R.C. Dorf, ed., second ed. CRC Press, 2006.

[21] A. von Meier, *Electric Power Systems: A Conceptual Introduction*, first ed. Wiley-IEEE Press, 2006.

[22] M. Erol-Kantarci and H. Mouftah, "Wireless Sensor Networks for Cost-Efficient Residential Energy Management in the Smart Grid," *IEEE Trans. Smart Grid*, vol. 2, no. 2, pp. 314-325, June 2011.

[23] A. Mohsenian-Rad, V. Wong, J. Jatskevich, R. Schober, and A. Leon-Garcia, "Autonomous Demand-Side Management Based on Game-Theoretic Energy Consumption Scheduling for the Future Smart Grid," *IEEE Trans. Smart Grid*, vol. 1, no. 3, pp. 320-331, Dec. 2010.

[24] A. Molderink, V. Bakker, M. Bosman, J. Hurink, and G. Smit, "Management and Control of Domestic Smart Grid Technology," *IEEE Trans. Smart Grid*, vol. 1, no. 2, pp. 109-119, Sept. 2010.

[25] M. Pedrasa, T. Spooner, and I. MacGill, "Coordinated Scheduling of Residential Distributed Energy Resources to Optimize Smart Home Energy Services," *IEEE Trans. Smart Grid*, vol. 1, no. 2, pp. 134-143, Sept. 2010.

[26] C. Ibars, M. Navarro, and L. Giupponi, "Distributed Demand Management in Smart Grid with a Congestion Game," *Proc. First IEEE Int'l Conf. Smart Grid Comm.*, pp. 495-500, Oct. 2010.

[27] K. Turitsyn, N. Sinitsyn, S. Backhaus, and M. Chertkov, "Robust Broadcast-Communication Control of Electric Vehicle Charging," *Proc. First IEEE Int'l Conf. Smart Grid Comm.*, pp. 203-207, Oct. 2010.

[28] C. de Morsella, "Wind Turbines May be Shut Down in Pacific Northwest," Green Economy Post, http://greeneconomypost.com/wind-turbines-shut-pacific-northwest-15566.htm, May 2011.

[29] *Available Transfer Capability Definitions and Determination*. North Am. Electric Reliability Council, http://www.westgov.org/wieb/wind/06-96NERCatc.pdf, June 1996.

[30] C. Barbulescu, S. Kilyeni, D. Cristian, and D. Jigoria-Oprea, "Congestion Management Using Open Power Market Environ-ment Electricity Trading," *Proc. 45th Int'l Univ. Power Eng. Conf. (UPEC)*, pp. 1-6, Sept./Oct. 2010.

[31] M. Ramezani, M.-R. Haghifam, C. Singh, H. Seifi, and M. Moghaddam, "Determination of Capacity Benefit Margin in Multiarea Power Systems Using Particle Swarm Optimization," *IEEE Trans. Power Systems*, vol. 24, no. 2, pp. 631-641, May 2009.

[32] M. bin Othman, A. Mohamed, and A. Hussain, "Determination of Transmission Reliability Margin Using Parametric Bootstrap Technique," *IEEE Trans. Power Systems*, vol. 23, no. 4, pp. 1689-1700, Nov. 2008.

[33] F. Jiang, "Investigation of Solar Energy for Photovoltaic Applica-tion in Singapore," *Proc. Int'l Power Eng. Conf. (IPEC)*, pp. 86-89, Dec. 2007.

[34] *Solar Electricity Basics*, Homepower, http://homepower.com/basics/solar/#SolarElectricPanels, 2012.

[35] A. Pandey, N. Dasgupta, and A. Mukerjee, "High-Performance Algorithms for Drift Avoidance and Fast Tracking in Solar MPPT System," *IEEE Trans. Energy Conversion*, vol. 23, no. 2, pp. 681-689, June 2008.

[36] *AC Disconnect Switches for Inverter-Based Generation*, Pacific Gas and Electric Company, http://www.pge.com/b2b/newgenerator/acdisconnectswitches/, 2012.

[37] C. Lo and N. Ansari, "The Progressive Smart Grid System from Both Power and Communications Aspects," *IEEE Comm. Surveys and Tutorials*, to appear.

[38] *Wireless LAN Medium Access Control (MAC) and Physical Layer (PHY) Specifications*, IEEE Std. 802.11, http://grouper.ieee.org/groups/802/11/, 2007.

[39] *Wireless Medium Access Control (MAC) and Physical Layer (PHY) Specifications for Low-Rate Wireless Personal Area Networks (LR-WPANs)*, IEEE Std. 802.15.4, http://grouper.ieee.org/groups/802/15/, 2006.

[40] *Smart e-meter: AMR/AMI*, Texas Instruments, http://focus.ti.com/docs/solution/folders/print/407.html, 2012.

[41] H. Kellerer, U. Pferschy, and D. Pisinger, *Knapsack Problems*, first ed. Springer, 2004.
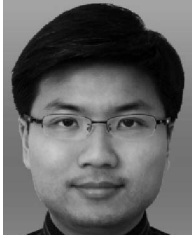
Chun-Hao Lo (S'08) received the BS degree in electrical and computer engineering from the Ohio State University, Columbus, in 2003, the MS degree in engineering from the University of Detroit Mercy, MI, in 2004, and the MS degree in telecommunications from New Jersey Institute of Technology (NJIT), Newark, in 2006. He is currently working toward the PhD degree in electrical engineering at NJIT. His research interests include smart grid systems, wireless communications, distributed control, and optimization. He is a student member of the IEEE.

Nirwan Ansari (S'78-M'83-SM'94-F'09) received the BSEE (summa cum laude with a perfect GPA) degree from the New Jersey Institute of Technology (NJIT), Newark, in 1982, the MSEE degree from the University of Michigan, Ann Arbor, in 1983, and the PhD degree from Purdue University, West Lafayette, IN, in 1988. He joined the NJIT's Department of Electrical and Computer Engineering as an assistant professor in 1988, became a tenured associate professor in 1993, and has been a full professor since 1997. He has also assumed various administrative positions at NJIT. He was a visiting (chair) professor at several universities. He authored *Computational Intelligence for Optimization* (Springer, 1997) with E.S.H. Hou and edited *Neural Networks in Telecommunications* (Springer, 1994) with B. Yuhas. He has also contributed more than 400 technical papers, more than one third of which were published in widely cited refereed journals/magazines. He has also guest edited a number of special issues, covering various emerging topics in communications and networking. His current research focuses on various aspects of broadband networks and multimedia communications. He has served on the Editorial Board and Advisory Board of eight journals, including as a senior technical editor of the *IEEE Communications Magazine* (2006-2009). He has served the IEEE in various capacities such as chair of the IEEE North Jersey Communications Society (COMSOC) Chapter, chair of the IEEE North Jersey Section, member of the IEEE Region 1 Board of Governors, chair of the IEEE COMSOC Networking Technical Committee Cluster, chair of the IEEE COMSOC Technical Committee on Ad Hoc and Sensor Networks, and Chair/Technical Program Committee Chair of numerous conferences/symposia. Some of his recent recognitions include a 2007 IEEE Leadership Award from the Central Jersey/Princeton Section, NJIT Excellence in Teaching in Outstanding Professional Development in 2008, a 2008 IEEE MGA Leadership Award, the 2009 NCE Excellence in Teaching Award, a couple of best paper awards (IC-NIDC 2009 and IEEE GLOBECOM 2010), a 2010 Thomas Alva Edison Patent Award, and designation as an IEEE Communications Society Distinguished Lecturer (2006-2009, two terms). He was also granted 15 US patents. He is a fellow of the IEEE.

▷ **For more information on this or any other computing topic, please visit our Digital Library at** www.computer.org/publications/dlib.